Polymer 52 (2011) 5503–5512

Contents lists available at SciVerse ScienceDirect

Polymer

journal homepage: www.elsevier.com/locate/polymer

Controlling the tacticity in the polymerization of N-isopropylacrylamide: A computational study

T. Furuncuoğlu Özaltın [a], İ. Değirmenci [a], V. Aviyente [a,*], C. Atılgan [b], B. De Sterck [c], V. Van Speybroeck [c], M. Waroquier [c]

[a] Department of Chemistry, Boğaziçi University, 34342 Bebek, İstanbul, Turkey
[b] Faculty of Engineering and Natural Sciences, Sabancı University, Orhanlı 34956, Tuzla, İstanbul, Turkey
[c] Center for Molecular Modeling, Ghent University-Member of the QCMM-Alliance Ghent-Brussels, Technologiepark 903, 9052 Zwijnaarde, Belgium

ARTICLE INFO

Article history:
Received 24 July 2011
Received in revised form
2 October 2011
Accepted 3 October 2011
Available online 10 October 2011

Keywords:
NIPAM
Modeling
Tacticity

ABSTRACT

In this study, the effect of alcohols as solvents on the kinetics and the tacticity of poly(N-Isopropylacrylamide) (PNIPAM) is investigated with a combined static and molecular dynamics set of computational tools. Classical molecular dynamics calculations have been carried out to determine the location of the solvent molecules in the proximity of the monomer and the dimer. A combined implicit/explicit solvent model was used for the evaluation of the kinetics of the dimeric polymer chains. Rate constants are calculated with the B3LYP/6-311 + G(d,p)//B3LYP/6-31 + G(d), BMK/6-311 + G(d,p)//B3LYP/6-31 + G(d), and MPWB1K/6-311 + G(d,p)//B3LYP/6-31 + G(d) methodologies via the standard transition state theory. We show that due to the proximity of the −NH and carbonyl groups on the syndiotactic propagating dimeric and trimeric chains, the alcohol can stabilize the corresponding transition states by forming a bridge between these functionalities and accelerate this path more than its isotactic counterpart. In agreement with experiment, the increase in the syndiotactic PNIPAM and the acceleration of the reaction in the presence of *t*-BuOH is predicted with all the DFT functionals utilized in this study.

1. Introduction

Free radical polymerization is one of the most favorable chemical reactions employed in industry, because it is possible to obtain high molecular weight polymeric materials from a wide variety of vinyl monomers without extensive purification [1]. Recently, living/controlled radical polymerization gained great attention since the control of highly active neutral radical species is very difficult. They undergo very fast propagation and termination steps generating dead chains [2]. Living/controlled radical polymerization has enabled obtaining well-defined polymers with controlled molecular weights [3]. However, besides the molecular weight, the tacticity of the growing chain should be controlled during the free radical polymerization. This is because, tacticity is a measure of stereoregularity of a polymer chain and many of the polymer properties such as tensile strength, melting point, and solubility depend on it [4]. There are two fundamental approaches for stereochemical control of polymers during free radical polymerization: (1) Catalytic control of the propagating chain end using Lewis acids, solvents, and chiral auxiliaries, and (2) use of polymerizations in organized and constrained media [5].

Recently, N-Isopropylacrylamide (NIPAM) (Fig. 1a) has attracted great attention because its polymer, Poly(N-Isopropylacrylamide) (PNIPAM) (Fig. 1b) has a lower critical solution temperature around human body temperature (LCST = 32 °C) [6]. LCST is the critical temperature where the polymer shows a phase transition due to the alterations in the hydrogen bonding interactions of the amide group. Since the hydrophobic interactions are favored above the critical temperature, the polymer collapses, whereas its hydrophilic end expands below the LCST [7,8]. This behavior makes PNIPAM a good candidate for the synthesis of hydrogels, drug delivery devices, reaction catalysis, and protein folding [8–10]. Recently, by using a simultaneous chain- and step-growth radical polymerization of NIPAM, tunable thermo-responsivity and degradability of the polymer product was obtained [11].

Tacticity strongly influences the solution property of PNIPAM. It was reported that PNIPAM with isotactic content over 72% was insoluble in water, whereas the atactic one showed a phase transition around 32 °C. As the syndiotactic content increased from 53 to 71%, T_c (the cloud point) increased from 33.1 to 35.9 °C [12]. Also, in another study, the importance of stereoregularity on the

* Corresponding author. Tel.: +90 2123596670; fax: +90 2122872467.
E-mail address: aviye@boun.edu.tr (V. Aviyente).

0032-3861/$ – see front matter © 2011 Elsevier Ltd. All rights reserved.
doi:10.1016/j.polymer.2011.10.009

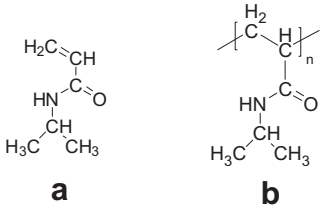

Fig. 1. Structures of (a) NIPAM and (b) PNIPAM.

solubility and the cloud point of PNIPAM in water was shown. According to this study, syndiotactic-rich PNIPAM samples were soluble in water and had higher cloud points and T_g (glass transition temperature) values compared to the isotactic-rich and atactic samples [13]. Several studies have been carried out in the literature to control the stereochemistry of PNIPAM during free radical polymerization [14,15]. Hirano et al. showed that the presence of pyridine N-oxide (PNO) induced isotacticity in the radical polymerization of NIPAM [14,15]. Also, they have found that stereocontrol can be achieved under metal-free conditions by forming hydrogen-bond-assisted complexes with NIPAM and Lewis bases like hexamethylphosphoramide (HMPA) which induced syndiotacticity [16]. Because PNIPAM is a thermo-responsive polymer, not only the hydrogen bond assistance, but also the temperature affects the final properties of the polymer [15,17]. It was reported that some simple alkyl alcohols such as methanol, *t*-butanol, and 3-methyl-3-pentanol played dual roles in the polymerization system by increasing the formation of syndiotactic specific PNIPAM, and accelerating the polymerization reaction [12]. According to this experimental study, the stereoregularity of the polymers in radical polymerization is achieved by the addition of simple alkyl alcohols. It was claimed that coordination of the alcohols with the −NH proton induced syndiotactic specificity, and H-bonding interaction with the C═O oxygen accelerated the reaction.

The majority of published computational studies for free radical polymerization have treated solvation by using simple continuum models, such as CPCM (Conductor-like Polarizable Continuum Model) [18] and PCM (Polarizable Continuum Model) [19], in which each solute molecule is simply embedded in a cavity surrounded by the relevant dielectric continuum [20]. Although these computationally efficient models also include additional terms for the non-electrostatic contributions of the solvent, such as dispersion, repulsion, and cavitation, they are generally thought to be reliable only when explicit solute–solvent interactions (such as hydrogen bonding) can be neglected [21–23]. Implicit/explicit solvent models [24] have been used with success as in the case of phosphate hydrolysis [25], however there are very few such studies for free radical polymerization reactions. Recently some of the authors have successfully used this methodology in the free radical polymerization of acrylamide (AA) and methacrylamide (MAA) [26]. Coote et al. have obtained accurate rate values for the propagation rate coefficients of acrylic and vinyl esters via a thermodynamic cycle in which accurate G3(MP2)-RAD calculations in the gas phase are corrected to the solution phase using free energies of solvation, as computed by the COSMO-RS method [27]. Recently, the SMD (Solvation Model Density) model [28] has gained great attention and is recommended for computing free energies of solvation. It is parametrized for any electronic structure method for which the PCM algorithm is available. It employs the radii and non-electrostatic terms optimized for the IEFPCM (Integral-Equation-Formalism Polarizable Continuum Model) algorithm. Very recently, it has been used successfully for the prediction of the effect of solvent polarity on the thermal isomerization of 3-methyl-4-pyrimidinimine [29]. The SMD model has been employed for the calculation of pK_a values of some oxicam derivatives, but gave less satisfactory results compared with the CPCM-UAKS and COSMO-RS models [30]. Nevertheless, it properly predicts the solvation free energies of peptides in water [31].

In this study, methanol has been chosen as a representative alkyl alcohol to understand the dual role of alkyl alcohols as syndiotactic-specificity inducers and accelerators. Classical molecular dynamics (MD) simulations are used to determine the preferential coordination sites of methanol molecules with the dimeric and the trimeric PNIPAM. Then, a combined implicit/explicit model is used to determine the full reaction kinetics of the dimeric PNIPAM as in other organic chemistry problems [32–34]. Furthermore, the effect of a bulkier alcohol, *t*-BuOH, on the acceleration of the rate of polymerization and on the increase in the syndiotacticity of PNIPAM is highlighted.

2. Methodology and computational procedure

In this study, the propagation reaction of PNIPAM is modeled as shown in Fig. 2. The structure of the propagating NIPAM radical (NIPAMR) is considered by replacing the long polymer chain with a radical derived from the attack of $CH_3\cdot$ to NIPAM. The reaction proceeds by the successive attacks of the newly formed radical species to monomers generating the propagating polymer chain (propagation reaction). As mentioned earlier in previous studies on chain length dependency of the propagation rate coefficient [35] and in some of our earlier studies [36], short propagating chains of the polymeric species can be used to have an insight on the qualitative trend of the reaction.

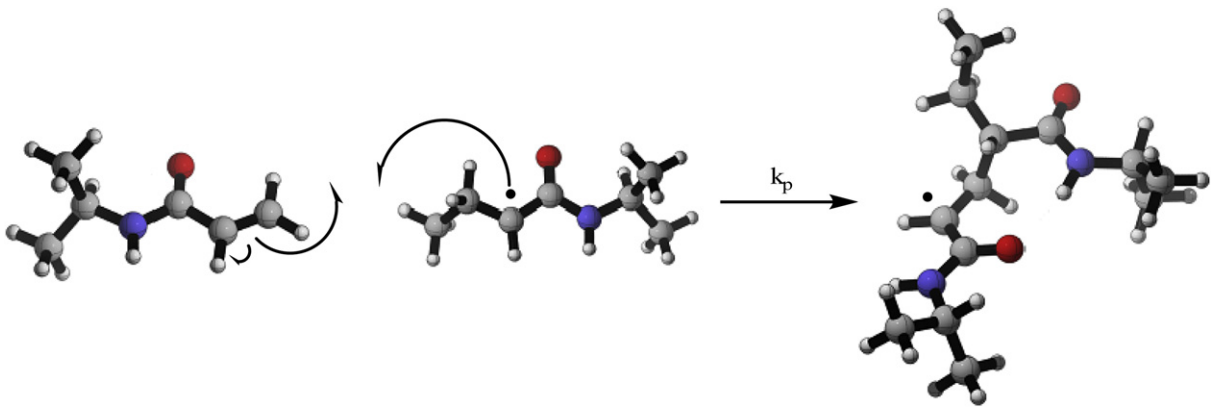

Fig. 2. Model for the propagation reaction of PNIPAM.

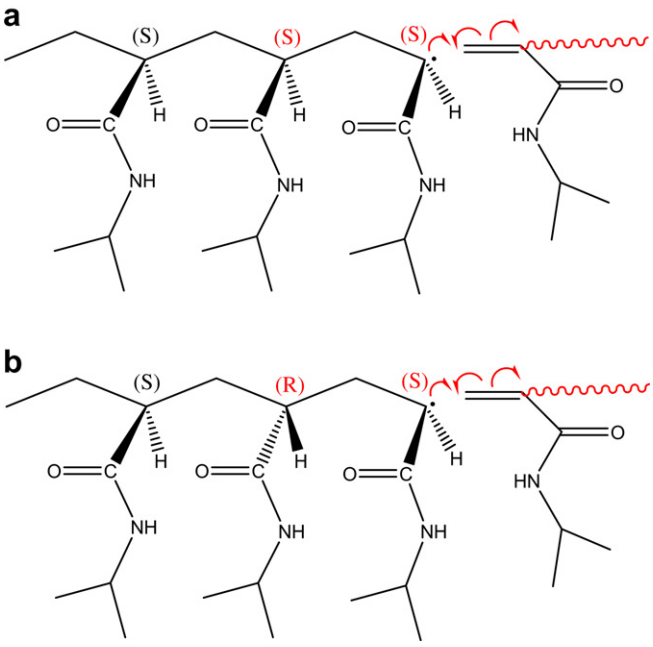

Fig. 3. Representation of (a) isotactic (b) syndiotactic transition states.

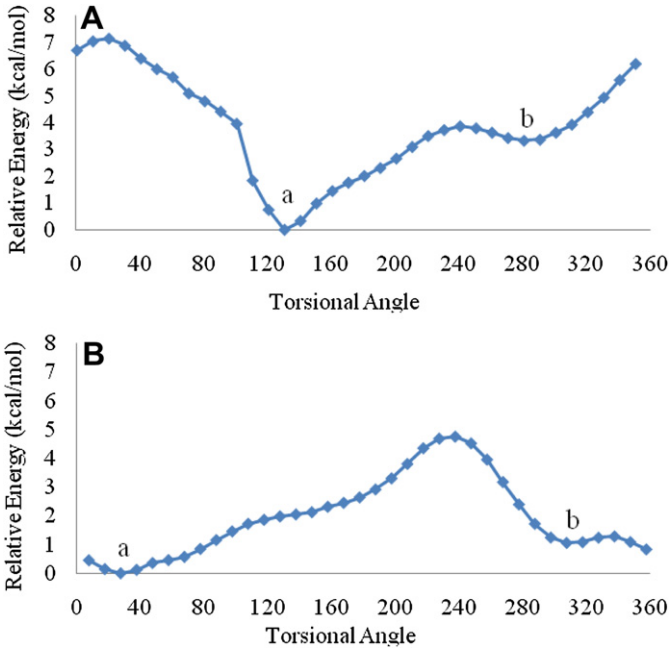

Fig. 5. Potential energy scans for isotactic (A) and syndiotactic (B) transition states (B3LYP/6-31 + G(d)).

Density Functional Theory (DFT) with the Gaussian03 program package [37] was used for most of the calculations. As in our previous studies on free radical polymerization, geometry optimizations were carried out with the B3LYP/6-31 + G(d) methodology [36b,36c,38]. For kinetic calculations at 300 K, the B3LYP/6-311 + G(d,p)//B3LYP/6-31 + G(d), BMK/6-311 + G(d,p)//B3LYP/6-31 + G(d), MPWB1K/6-311 + G(d,p)//B3LYP/6-31 + G(d) methodologies have been used. Among these functionals, BMK [39] is recommended for the calculation of transition state barriers, MPWB1K [40] is known to be successful for thermochemistry, thermochemical kinetics, hydrogen bonding, and weak interactions. The Gaussian09 program package [41] was used for calculations with the SMD model.

2.1. Calculations in the gas phase

The conformational analysis of the species reported in this study was performed with the B3LYP/6-31 + G(d) methodology. For each

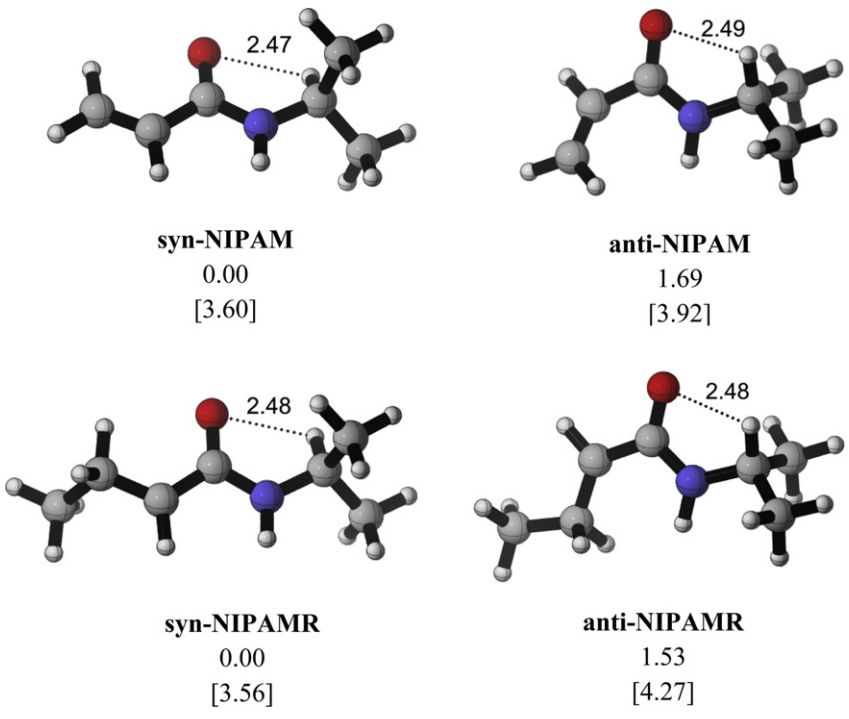

Fig. 4. Relative electronic energies (with zero point energy correction) (B3LYP/6-31 + G(d), kcal/mol) of monomers and radicals and dipole moments (D) in square brackets.

of the species, rotation around single bonds was conducted to determine the most stable conformers. The best conformers for NIPAM and its propagating radical NIPAMR were used for the construction of the transition states. The tacticity of the propagating radical was taken into account as displayed in Fig. 3.

The propagating chain was initiated by attack of a methyl radical to NIPAM. The radical thus formed would attack another NIPAM monomer via a transition structure yielding either an isotactic or a syndiotactic polymer chain. Since earlier studies have shown the importance of accounting for the most stable transition states, a relaxed potential energy scan was performed around the forming critical bond of the structures corresponding to transition states in order to locate their best conformations [38a,38b,42]. The stationary points located in this manner were used for further analyses. IRC calculations with the B3LYP/6-31 + G(d) methodology were performed to justify the nature of the transition states [43].

2.2. Calculations in solution

In this study, the effect of the solvent on the tacticity of PNIPAM was calculated in two ways:

(1) The free radical polymerization of PINAM in toluene was considered by using the SMD (Solvation Model Density) implicit solvation model [28].
(2) The free radical polymerization in toluene and methanol was modeled by using a mixed implicit/explicit solvation model. For this purpose the location of methanol around NIPAM and dimeric PNIPAM species was found by performing classical MD simulations (as outlined in the next subsection). Once the coordination sites of methanol around the dimeric PNIPAM were established, similar transition structures (monomer + radical leading to dimers) were located and soaked into toluene described as continuum. Implicit solvent calculations were carried out with

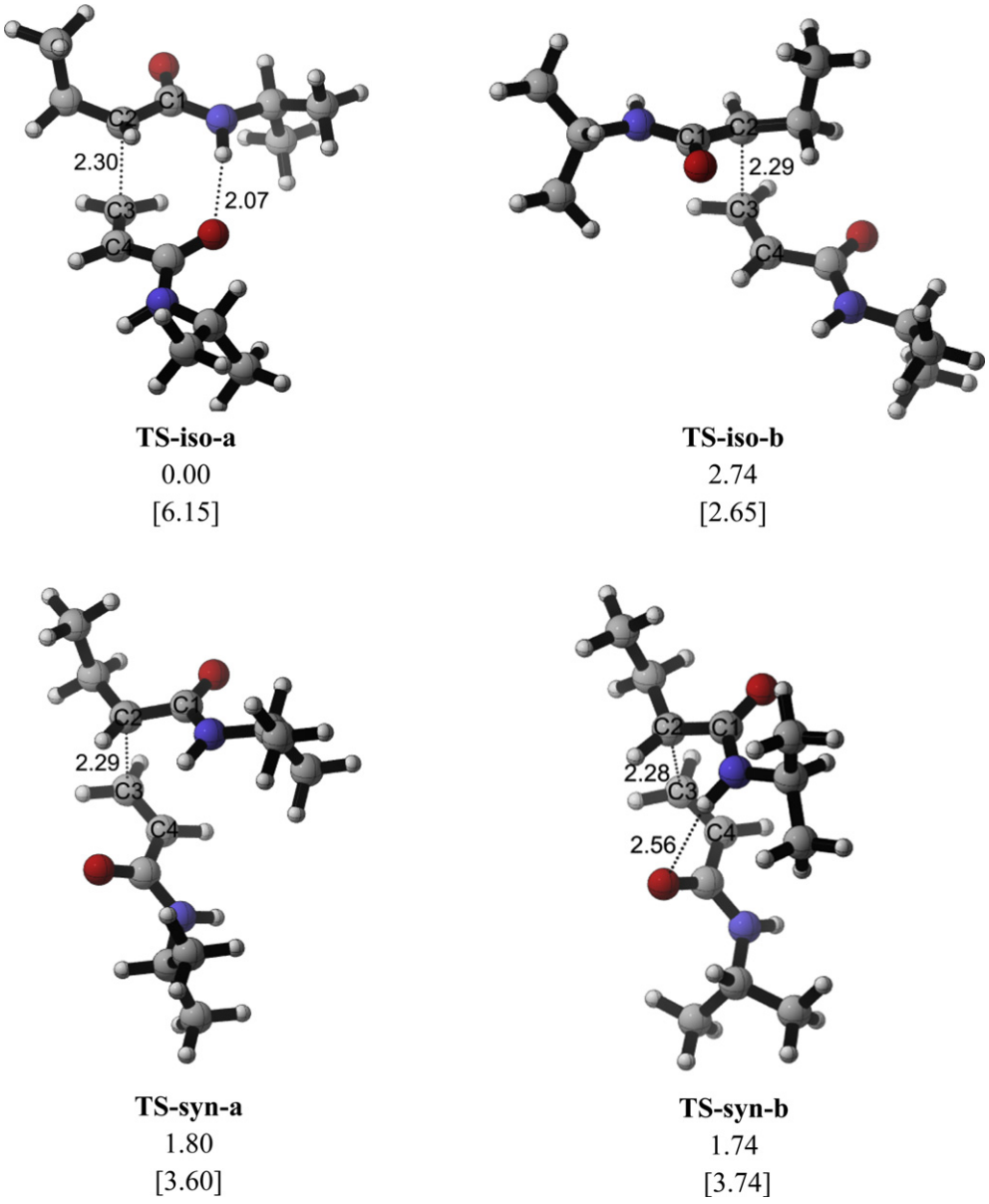

Fig. 6. Relative electronic energies (with zero point energy correction) (B3LYP/6-31 + G(d), kcal/mol) of the transition structures and dipole moments (D) in square brackets.

the SMD solvation model for the formation of syndiotactic and isotactic dimeric PNIPAM. The same procedure was followed for including *t*-BuOH explicitly in the reaction.

2.3. MD simulations

MD simulations were carried out on the monomer of NIPAM, as well as on the isotactic and syndiotactic dimeric and trimeric chains of PNIPAM. Each of these systems was separately soaked in the solvent of toluene/methanol mixture. Experimentally, excess alcohol has been used to induce syndiotactic-specificity [12]. The polymerization reaction is performed with 0.5 mol/L NIPAM monomer and 2.0 mol/L methanol in 1 L of toluene (~10 mol) solution. For the target mixture, a solution with a density of 1.04 g/cm^3 corresponding to that of the experimentally studied system was used [12]. MD runs were performed for both the isotactic and the syndiotactic dimeric and trimeric products in the presence of toluene as a continuum and with 1:4 monomer:methanol ratio. Each simulation box thus contains three molecules of NIPAM (PNIPAM-dimer or PNIPAM-trimer), 12 methanol and 60 toluene molecules. Each side of the cubic boxes is 21.53 Å for monomeric NIPAM, 21.97 Å for the dimers of PNIPAM and 22.26 Å for the trimers of PNIPAM. The boxes were constructed with the Amorphous Cell module of Accelrys Materials Studio suite of programs [44]. COMPASS forcefield [45] was used with a cutoff distance of 10 Å, and a switching function with spline and buffer widths of 1.0 and 0.5 Å, respectively. Periodic boundary conditions were imposed on the systems which are initially subjected to 5000 steps of conjugate gradients minimization up to a convergence of 1 kcal/mol/Å. MD simulations were perfomed in the NVT ensemble at 298 K using the Andersen thermostat as the temperature control method with a collision ratio of 1.0 [46]. Equilibration MD runs were carried out for 200 ps followed by production runs of 1 ns length each. The time step was set to 1 fs and coordinates from the production stage were recorded every 1 ps for further analysis. Thus, all the conformational analyses presented are based on 1000 snapshots.

At the end of the simulations, most frequently observed frames, having a product stabilized by a methanol molecule, were chosen. These were converted to transition state structures by breaking the critical forming bond, and omitting terminal hydrogen. Geometry optimizations with B3LYP/6-31 + G(d) were performed on these initial transition structures. The ones having the lowest free energy of activation were chosen as the best conformers in the presence of explicit methanol molecules and used for the kinetic calculations with density functional theory. Similar structures have been constructed with *t*-BuOH.

2.4. Kinetics

After choosing the best conformers for the transition states and performing kinetic calculations with DFT, reaction rates are calculated by using transition state theory, for which the rate constant is given by:

$$k_2 = k\frac{kT}{h}\frac{RT}{p^{\theta}}e^{-\Delta G^{\ddagger}/RT}$$

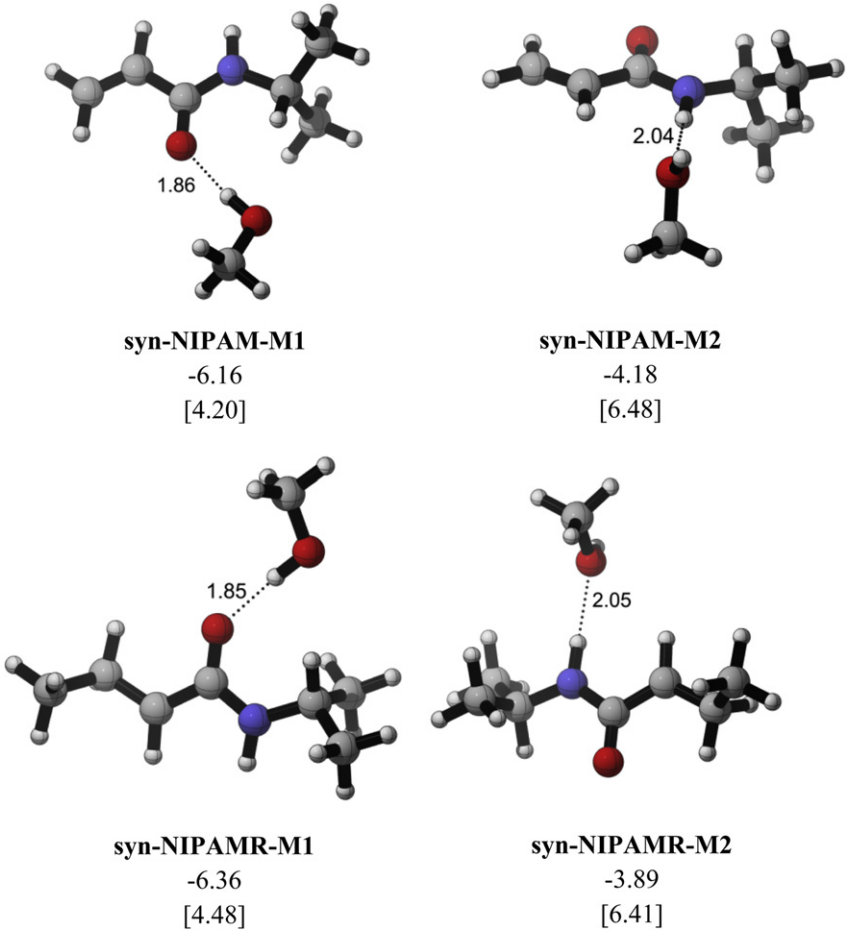

Fig. 7. Stabilization energies (B3LYP/6-31 + G(d), kcal/mol) and dipole moments (D) in square brackets for **NIPAM-CH$_3$OH** and **NIPAMR-CH$_3$OH**.

where k represents Boltzmann's constant, T is the temperature, h is Planck's constant, $\Delta G^{\ddagger}$ represents the molecular Gibbs Free energy difference between the activated complex and the reactants (with inclusion of zero point vibrational energies), R is the universal gas constant, κ is the transmission coefficient which is assumed to be about 1 and p^{θ} is the standard pressure 10^5 Pa (1 bar) [47].

At each level of theory (LOT), the Gibbs Free energies of each species in solution are obtained as the sum of the corresponding gas-phase thermal corrections to the Gibbs free energy, the calculated free energy of solvation with non-electrostatic effects, and a correction term, RT ln(24.46), to take account the passage from 1 mol/L(g) to 1 mol/L(soln) [48].

3. Results

3.1. Conformational study of the propagating species in vacuum

3.1.1. NIPAM and NIPAMR

The conformational analysis showed that the *syn* conformer of the monomer, **syn-NIPAM**, is more stable than the *trans* conformer **anti-NIPAM** by 1.69 kcal/mol. The relative stability of **syn-NIPAM** as compared to **anti-NIPAM** may be attributed to its extended chain as well as to its smaller dipole moment (3.60 D for **syn-NIPAM** compared to 3.92 D for **anti-NIPAM**). Based on similar considerations **syn-NIPAMR** (3.56 D) is more stable than **anti-NIPAMR** (4.27 D). Notice that in all of these structures, there is a stabilizing interaction between one of the hydrogen atoms of the isopropyl group and the carbonyl oxygen (Fig. 4).

3.1.2. Transition states

In the transition structures, the attack of the most stable radical (**syn-NIPAMR**) to the most stable monomer (**syn-NIPAM)** was considered. The potential energy scan was performed along the critical bond (C•—C(C═C)) and two stationary points were found for both types of transition states (Fig. 5). The structures corresponding to minima (a and b) on the potential energy surfaces of the isotactic and syndiotactic transition states were further optimized (Fig. 6).

TS-iso-a (C1-C2-C3-C4 = 130.7°) has a stabilizing interaction between the N-H proton of the radical and the carbonyl oxygen of the monomer (2.07 Å) and is more stable than **TS-iso-b** (C1-C2-C3-C4 = 284.2°) by 2.74 kcal/mol in terms of electronic energy in spite of its high dipole moment. This behavior may be attributed to the stabilizing effect of H-bonding in **TS-iso-a.** Also note that this is the earliest transition structure.

The structures corresponding to the two minima (a and b) on the potential energy surface of the syndiotactic transition structures are very close in energy to each other: **TS-syn-a** (C1-C2-C3-C4 = 48.1°) is extended while **TS-syn-b** (C1-C2-C3-C4 = 29.2°) is hindered, but slightly stabilized by H-bonding interactions (Fig. 6). Overall, due to stabilizing H-bonding interactions, **TS-iso-a** is the most stable transition structure in the gas phase despite its high dipole moment.

3.1.3. NIPAM and NIPAMR with explicit methanol molecules

The location of explicit methanol molecules on the reacting species is crucial in evaluating the tacticity and the kinetics of the free radical propagation of PNIPAM in the presence of methanol. In the MD simulations only one methanol molecule was found to be in

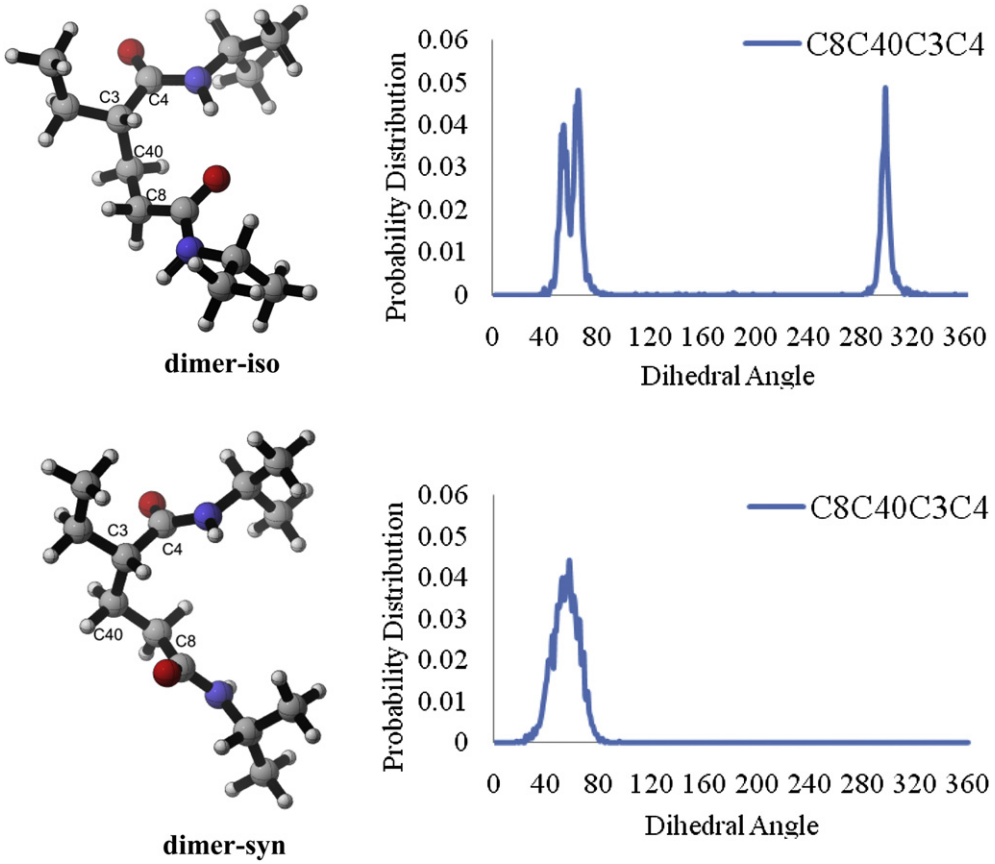

Fig. 8. Probability distribution for syndiotactic and isotactic dimeric **NIPAM** chains in the MD simulation box.

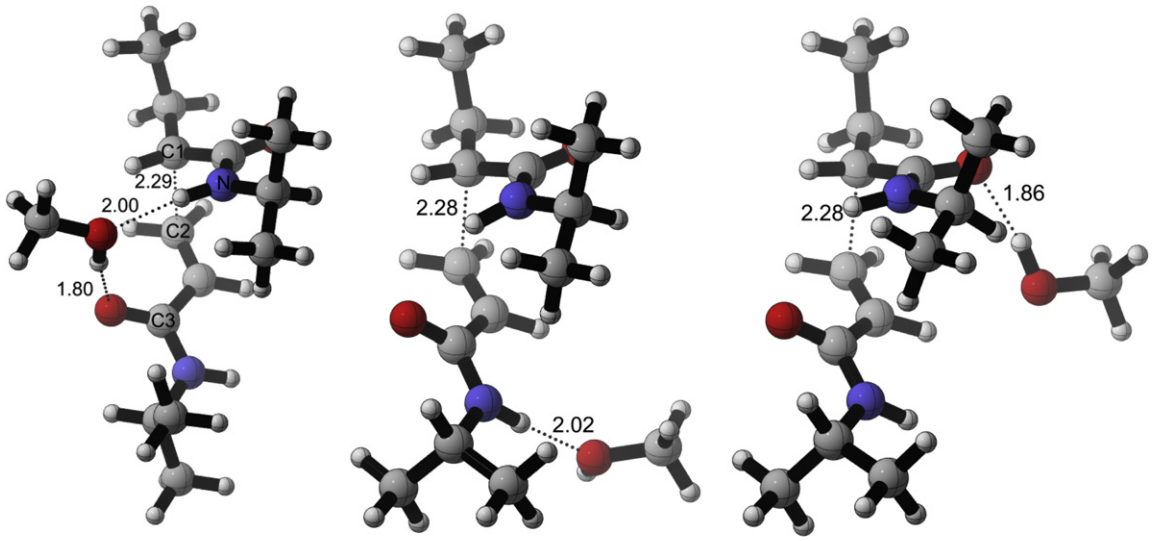

TS-syn-M1
-10.13
[3.90]

TS-syn-M2
-4.45
[5.21]

TS-syn-M3
-7.56
[1.54]

Fig. 9. Stabilization energies (B3LYP/6-31 + G(d), kcal/mol) and dipole moments (D) in square brackets for syndiotactic transition states with one explicit methanol molecule.

close proximity to NIPAM in spite of the excess methanol (4–1) introduced in the MD box. The probability distribution analysis has revealed that hydrogen bonding interaction with the carbonyl oxygen was observed more frequently than with the N–H proton. NIPAM-methanol complexes were located for both types; stabilization energies of the methanol-NIPAM or methanol-NIPAMR complexes were calculated as the difference of the electronic energies (with the inclusion of zero point energy correction) of the molecule–methanol complex, the molecule and the solvent. Conformers where the O–H proton of methanol and the carbonyl oxygen are stabilized through a hydrogen bond are found to be more stable than the others (Fig. 7).

In structures where methanol coordinates to the carbonyl oxygen (**syn-NIPAM-M1**, **syn-NIPAMR-M1**) the hydrogen bond distances are shorter than in the other cases; strong hydrogen bonds render these structures more stable than the others. Also note that these structures have low dipole moments due to the opposite orientation of the carbonyl groups; comparison of the stabilization energies of **syn-NIPAM-M1** and **syn-NIPAMR-M1** shows that the latter is slightly more stabilized by methanol (Fig. 7).

3.1.4. *Transition states with explicit methanol molecules*

As mentioned earlier in the Methodology section, MD simulations have been performed on the dimeric chains (isotactic and syndiotactic) to determine the location of methanol in the vicinity

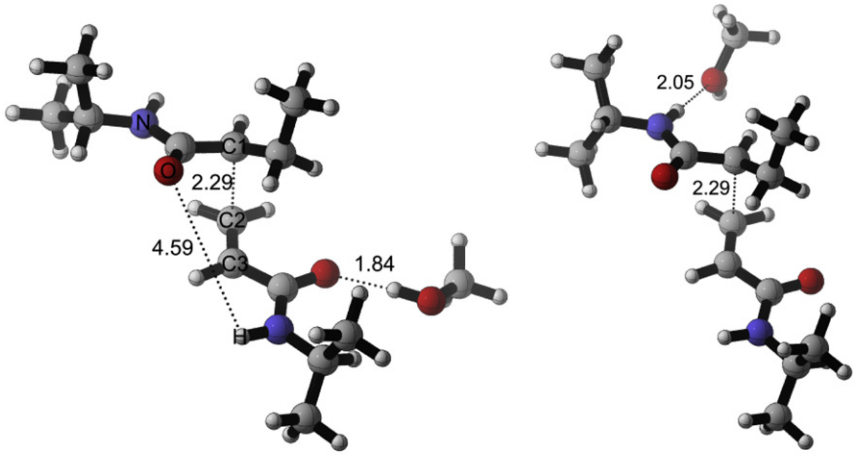

TS-iso-M1
-6.52
[4.86]

TS-iso-M2
-4.17
[4.25]

Fig. 10. Stabilization energies (B3LYP/6-31 + G(d), kcal/mol) and dipole moments (D) in square brackets for isotactic transition states with one explicit methanol molecule.

Table 1
Activation energy barriers ($\Delta E^{\#}$, kcal/mol), Gibbs free energy barriers ($\Delta G^{\#}$, kcal/mol), propagation rate constants (k_p, m^3/mol s) for the dimeric PNIPAM chain.

		B3LYP[a]			**BMK**[b]			**MPWB1K**[c]		
		No alcohol	1 MeOH	1 *t*-BuOH	No alcohol	1 MeOH	1 *t*-BuOH	No alcohol	1 MeOH	1 *t*-BuOH
$\Delta E^{\#}_{(gas)}$	Iso	7.5	7.4	7.3	5.7	3.9	5.7	4.8	4.8	4.5
	Syn	6.9	3.2	2.9	5.1	1.7	1.2	3.8	0.5	−0.1
$\Delta G^{\#}_{(gas)}$	Iso	19.9	20.8	19.7	18.0	17.3	18.0	17.2	18.2	16.9
	Syn	18.9	18.4	17.0	17.2	16.9	15.3	15.9	15.7	14.0
$\Delta G^{\#}_{(toluene)}$	Iso	19.2	20.2	19.3	17.5	18.6	17.6	16.6	17.6	16.5
	Syn	18.2	19.1	17.8	16.7	17.7	16.2	15.4	16.4	14.9
$k_{p\ (toluene)}$	Iso	1.58E-03	3.09E-04	1.49E-03	2.67E-02	4.59E-03	2.32E-02	1.36E-01	2.35E-02	1.49E-01
	Syn	8.72E-03	1.99E-03	1.79E-02	1.09E-01	2.17E-02	2.57E-01	1.02E+00	1.73E-01	2.33E+00
%$_{(toluene)}$	Iso	16	14	7	21	18	9	12	12	6
	Syn	84	86	93	79	82	91	88	88	94
Average k_p $_{(toluene)}$		7.59E-03	1.76E-03	1.67E-02	9.19E-02	1.86E-02	2.37E-01	9.16E-01	1.55E-01	2.19E+00

(Iso = **TS-iso-b**; **TS-iso-M1** with methanol; **TS-iso-B** with *t*-BuOH; Syn = **TS-syn-a; TS-syn-M1** with methanol; **TS-syn-B** with *t*-BuOH).
[a] B3LYP/6-311 + G(d,p)//B3LYP/6-31 + G(d).
[b] BMK/6-311 + G(d,p)//B3LYP/6-31 + G(d).
[c] MPWB1K/6-311 + G(d,p)//B3LYP/6-31 + G(d).

of the propagating species. Analysis of the probability distributions of the dimers has shown that for **dimer-iso,** two structures predominate the others. These structures may be identified by monitoring the dihedral angle (C8C40C3C4) along the backbone: Two different structures corresponding to dihedral angles of 60° and 300° (similar to **TS-iso-b**) dominate throughout the 1000 recorded snapshots of the MD trajectory (Fig. 8). The syndiotactic dimer, **dimer-syn**, has a single conformation, which corresponds to the transition state **TS-syn-a.** None of the dimeric species in methanol had an intramolecular H-bonding interaction between their C═O oxygen and −NH proton as in **TS-iso-a** and **TS-syn-b**. Thus we have picked the backbones resembling **TS-syn-a** and **TS-iso-b** for further analysis.

For the syndiotactic dimeric species, **dimer-syn**, in MD simulations, a methanol molecule bridging the −NH and O═C groups of adjacent monomeric units was observed during 440 frames out of 1000 (Fig. 8). Structures for dimeric transition states with an explicit methanol molecule at various positions were located with B3LYP/6-31 + G(d) and their stabilization energies were calculated; that with the bridging methanol had the highest stabilization energy in agreement with the structure demonstrated by MD for the dimeric species. **TS-syn-M1** with a methanol molecule at the bridging position has been used for further kinetic calculations. As can be seen from Fig. 9, in the earliest transition structure **TS-syn-M1,** the −NH and C═O groups face each other (NC1C2C3 is 38°) favoring the formation of a methanol bridge.

In the isotactic dimeric species, **dimer-iso**, methanol was in close proximity either to the carbonyl oxygen or the −NH proton during the MD simulations. We have considered both types of complexation with **TS-iso-b**, have calculated their stabilization energies with respect to the separated reactants and have used the most stable transition structure, **TS-iso-M1** as a representative transition structure for the isotactic free radical polymerization of the dimer: in none of the frames did methanol occupy a bridging position. As can be seen from Fig. 10 the distance between the carbonyl oxygen of NIPAMR (O) and −NH proton of NIPAM (H) is around 4.59 Å. Furthermore, the two groups do not face each other (the NC1C2C3 dihedral angle is 136°) thus, a bridging position for methanol is not available.

3.2. Effect of methanol on the kinetics of the propagation reaction

Table 1 displays the energy barriers, $\Delta E^{\#}$, the Gibbs free energy barriers at 300 K, $\Delta G^{\#}$, the propagation rate constant, k_p, for the isotactic and syndiotactic dimeric PNIPAM in the gas phase and in solution. Solvent calculations were carried out with the SMD model by choosing toluene as a continuum as in the experimental study [12]. With B3LYP/6-311 + G(d,p)//B3LYP/6-31 + G(d) in vacuum

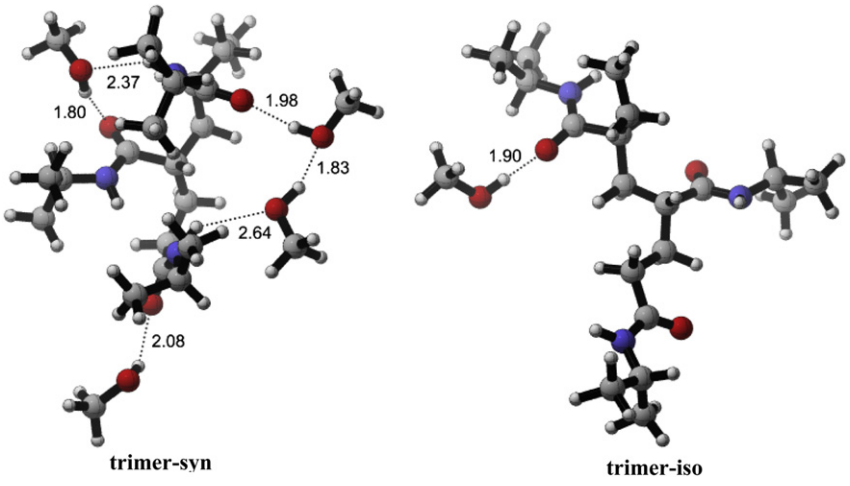

Fig. 11. Trimeric chains with methanol from MD simulations.

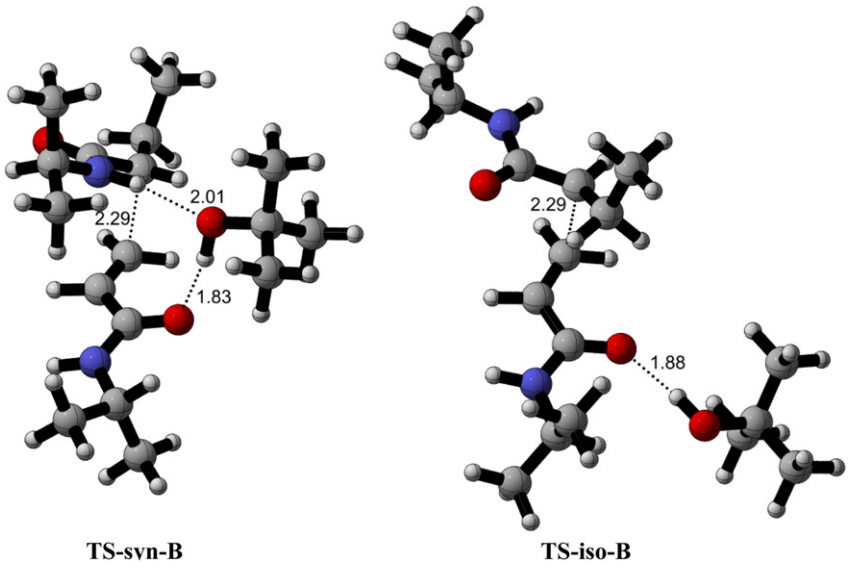

Fig. 12. Dimeric transition states with explicit *t*-BuOH.

without methanol, the activation energy barrier for the syndiotactic dimerization is slightly lower than the one for the isotactic case. However, the presence of methanol lowers the barrier considerably due to the stabilization of the syndiotactic chain via the methanol bridge. The Gibbs free energy barriers in vacuum display the same trend: the entropy of activation has a considerable contribution for this bimolecular reaction, and the presence of a methanol bridge in the syndiotactic transition state facilitates the propagation reaction. In solution, the propagation reaction is facilitated both for the isotactic and the syndiotactic cases. In **TS-syn-M1,** methanol coordinates with both –NH and C=O, whereas in the isotactic case, **TS-iso-M1**, there is an interaction only with the C=O oxygen of the monomer. As claimed in the experimental study [12], hydrogen bonding with the –NH proton induces the syndiotacticity. The experimental behavior is such that the r dyad content in PNIPAM at 0 °C is 53% in toluene with an increase to 61% in the presence of methanol [12]. Although the model used in this study for the propagating dimer is not expected to reproduce quantitatively the experimental results, it shows satisfactorily the increase in the syndiotactic product with the B3LYP/6-311 + G(d,p)//B3LYP/6-31 + G(d) and with the BMK/6-311 + G(d,p)//B3LYP/6-31 + G(d) methodologies. It is noteworthy to emphasize that purely due to the structure of the transition states of PNIPAM, (**TS-iso-M1** and**; TS-syn-M1**) a different solvation behavior is observed in each case. It is the bridging methanol that determines the increase in syndiotactic product formation, as justified by both the static and dynamic simulations.

To verify whether the trimeric chains show the same behavior as the dimeric ones, MD studies for the trimers were performed. Throughout the 1000 recorded snapshots of the MD trajectory, structures similar to **trimer-iso** have been observed in 193 frames out of 1000; structures similar to **trimer-syn** were observed in 200 frames out of 1000. The structure depicted in Fig. 11 for **trimer-syn** illustrates the presence of the methanol bridges, confirming the stabilization in the syndiotactic chain by methanol.

3.3. How does a bulkier alcohol affect the kinetics of the free radical polymerization?

To examine the effect of a bulkier alcohol on the rate of free radical polymerization of NIPAM, methanol molecules in **TS-syn-M1** and **TS-iso-M1** were replaced with *t*-BuOH and optimized with B3LYP/6-31 + G(d) to generate **TS-syn-B** and **TS-iso-B** (Fig. 12, Table 1). Acceleration in the presence of *t*-BuOH was confirmed with all the methodologies. The average value for k_p, calculated as the sum of the isotactic and the syndiotactic propagation rate constants multiplied with their population, increases in the presence of *t*-BuOH in line with the experimental behavior of PNIPAM [12]. The electronic energy barriers, $\Delta E^{\#}_{(gas)}$, with *t*-BuOH are comparable in magnitude with the ones with MeOH. However, the Gibbs free energy barriers, $\Delta G^{\#}_{(gas)}$ are lower with the bulkier alcohol indicating that the latter is favored entropically. Also note that there is a considerable increase in the syndiotactic PNIPAM in the presence of *t*-BuOH with all the methodologies: 84%–93% with B3LYP/6-311 + G(d,p)//B3LYP/6-31 + G(d); 79%–91% with the BMK/6-311 + G(d,p)//B3LYP/6-31 + G(d) and 88%–94% with MPWB1K/6-311 + G(d,p)//B3LYP/6-31 + G(d).

4. Conclusions

This study deals with the usage of both static and molecular dynamics computational tools in rationalizing the control of tacticity in the free radical polymerization of PNIPAM in the presence of methanol and *t*-butanol. Although the presence of hydrogen bonds between the propagating chain and the solvent is expected to lower activation barriers and accelerate the free radical polymerization of both syndiotactic and isotactic transition states leading to PNIPAM, modeling is necessary to understand the dual roles of alkyl alcohols as syndiotactic-specificity inducers and accelerators. MD followed by DFT calculations for the dimeric PNIPAM have revealed that in the syndiotactic free radical polymerization of NIPAM, the C=O and –NH groups are in closer proximity than in the isotactic chain, allowing the two sites to be bridged by a solvent molecule. The percentage of syndiotactic dimeric PNIPAM formation is higher in the presence of alkyl alcohols with all DFT functionals in agreement with experiment, justifying the usage of the dimeric-PNIPAM model and the methodology presented in this study. Average k_p values in toluene with all methodologies confirm that the presence of *t*-BuOH as a solvent in the free radical polymerization of PNIPAM accelerates the reaction, in agreement with the experimental behavior. Methanol in the vicinity of the syndiotactic trimeric-PNIPAM chains stabilizes these structures as in the case of dimeric-PNIPAM chains.

Acknowledgment

The computational resources used in this work were provided by Ghent University, the National Center for High Performance Computing of Turkey (UYBHM) under the grant number 20502009, and the TUBITAK ULAKBIM High Performance Computing Center. The UGent authors thank the FWO (Fonds voor Wetenschappelijk Onderzoek - Vlaanderen, Fund for Scientific Research - Flanders), the research board of Ghent University for the bilateral project Ghent – Istanbul and the IAP-BELSPO project in the frame of IAP 6/27 for financial support of this research.

Appendix. Supplementary material

Supplementary material associated with this article can be found, in the online version, at doi:10.1016/j.polymer.2011.10.009.

References

[1] Satoh K, Kamigaito M. Chem Rev 2009;109:5120–56.
[2] Moad G, Solomon DH. The chemistry of radical polymerization. 2nd ed. Oxford UK: Elsevier; 2006.
[3] Kamigaito M, Satoh K. J Polym Sci Part A Polym Chem 2006;44:6147–58.
[4] Porter NA, Allen TR, Breyer RA. J Am Chem Soc 1992;114:7676–83.
[5] Matyjaszewski K, Davis TP. Handbook of radical polymerization. Hoboken: Wiley-Interscience; 2002.
[6] Swanson L, Rimmer S, Soutar I. Polym Int 2009;58:273–8.
[7] Yin ZZ, Zhang JJ, Jiang LP, Zhu JJ. J Phys Chem C 2009;113:16104–9.
[8] Safrany A, Wojnarovits L. Rad Phys Chem 2003;67:707–15.
[9] Oupicky D, You YZ. Biomacromolecules 2007;8:98–105.
[10] Liu SY, Ge ZS, Xie D, Chen DY, Jiang XZ, Zhang YF, et al. Macromolecules 2007;40:3538–46.
[11] Kamigaito M, Mizuntani M, Satoh K. Macromolecules 2011;44:2382–6.
[12] Hirano T, Okumura Y, Kitajima H, Seno M, Sato T. J Polym Sci Part A Polym Chem 2006;44:4450–60.
[13] Ishizone T, Ito M. J Polym Sci Part A Polym Chem 2006;44:4832–45.
[14] Hirano T, Ishizu H, Seno M, Sato T. Polymer 2005;46:10607–10.
[15] Hirano T, Ishizu H, Sato T. Polymer 2008;49:438–45.
[16] Hirano T, Miki H, Seno M, Sato T. Polymer 2005;46:5501–5.
[17] Hirano T, Ishii S, Kitajima H, Seno M, Sato T. J Polym Sci Part A Polym Chem 2005;43:50–62.
[18] (a) Klamt A, Schuurmann G. J Chem Soc Perkin Trans 1993;2:799–805;
(b) Cossi M, Rega N, Scalmani G, Barone V. J Comput Chem 2003;24:669–81.
[19] Miertus S, Scrocco E, Tomasi J. Chem Phys 1981;55:117–29.
[20] Seabrook SA, Tonge MP, Gilbert RG. J Polym Sci Part A Polym Chem 2005;43:1357–68.
[21] Tomasi J. Theor Chem Acc 2004;112:184–203.
[22] Takano Y, Houk KN. J Chem Theory Comput 2005;1:70–7.
[23] Coote ML, Ho JM. J Chem Theory Comput 2009;5:295–306.
[24 (a) Pliego JR, Riveros JM. J Phys Chem A 2001;105:7241–7;
(b) Kelly CP, Cramer CJ, Truhlar DG. J Phys Chem A 2006;110:2493–9.
[25] Kamerlin SCL, Haranczyk M, Warshel A. Chem PhysChem 2009;10:1125–34.
[26] Van Speybroeck V, De Sterck B, Vaneerdeweg R, Du Prez F, Waroquier M. Macromolecules 2010;43:827–36.
[27] Coote ML, Lin CY, Izgorodina EI. Macromolecules 2010;43:553–60.
[28] Cramer CJ, Marenich AV, Truhlar DG. J Phys Chem B 2009;113:6378–96.
[29] Glaser R, Coyle S. J Org Chem 2011;76:3987–96.
[30] Coote ML, Ho JM, Franco-Perez M, Gomez-Balderas R. J Phys Chem A 2010;114:11992–2003.
[31] Kang YK, Byun BJ. J Comput Chem 2010;31:2915–23.
[32] Van Speybroeck V, De Sterck B, Mangelinckx S, Verniest G, De Kimpe N, Waroquier M. J Phys Chem A 2009;113:6375–80.
[33] Ha HJ, D'hooghe M, Catak S, Stankovic S, Waroquier M, Kim Y, et al. Eur J Org Chem; 2010:4920–31.
[34] De Kimpe N, D'hooghe M, Van Speybroeck V, Van Nieuwenhove A, Waroquier M. J Org Chem 2007;72:4733–40.
[35] (a) Heuts JPA, Gilbert RG, Radom L. Macromolecules 1995;28:8771–81;
(b) Wong MW, Radom L. J Phys Chem 1995;99:8582–8;
(c) Heuts JPA, Gilbert RG, Radom L. J Phys Chem 1996;100:18997–9006;
(d) Wong MW, Radom L. J Phys Chem A 1998;102:2237–45;
(e) Fischer H, Radom L. Angew Chem Int Ed 2001;40:1340–71;
(f) Gomez-Balderas R, Coote ML, Henry DJ, Fischer H, Radom L. J Phys Chem A 2003;107:6082–90;
(g) Gomez-Balderas R, Coote ML, Henry DJ, Radom L. J Phys Chem A 2004;108:2874–83;
(h) Henry DJ, Coote ML, Gomez-Balderas R, Radom L. J Am Chem Soc 2004;126:1732–40;
(i) Coote ML. Macromol Theory Simul 2009;18:388–400;
(j) Coote ML, Izgorodina EI. Chem Phys 2006;324:96–110.
[36] (a) Aviyente V, Degirmenci I, Eren S, De Sterck B, Hemelsoet K, Van Speybroeck V, et al. Macromolecules 2010;43:5602–10;
(b) Aviyente V, Degirmenci I, Avci D, Van Cauter K, Van Speybroeck V, Waroquier M. Macromolecules 2007;40:9590–602;
(c) Aviyente V, Degirmenci I, Van Speybroeck V, Waroquier M. Macromolecules 2009;42:3033–41;
(d) Gunaydin H, Salman S, Tuzun NS, Avci D, Aviyente V. Int J Quantum Chem 2005;103:176–89;
(e) Salman S, Albayrak AZ, Avci D, Aviyente V. J Polym Sci Part A Polym Chem 2005;43:2574–83.
[37] Frisch MJTGW, Schlegel HB, Scuseria GE, Robb MA, Cheeseman JR, Montgomery Jr JA, et al. Gaussian 03. Revision D.01. Wallingford CT: Gaussian. Inc.; 2004. Gaussian. Inc. Wallingford CT, 2004.
[38] (a) Van Cauter K, Van Speybroeck V, Vansteenkiste P, Reyniers MF, Waroquier M. ChemPhysChem 2006;7:131–40;
(b) Van Speybroeck V, Van Cauter K, Coussens B, Waroquier M. ChemPhysChem 2005;6:180–9;
(c) Coote ML. J Phys Chem A 2004;108:3865–72;
(d) Smith DM, Nicolaides A, Golding BT, Radom L. J Am Chem Soc 1998;120:10223–33;
(e) Aviyente V, Furuncuoglu T, Ugur I, Degirmenci I. Macromolecules 2010;43:1823–35.
[39] Boese AD, Martin JML. J Chem Phys 2004;121:3405–16.
[40] Zhao Y, Truhlar DG. J Phys Chem A 2004;108:6908–18.
[41] Frisch MJ, Trucks GW, Schlegel HB, Scuseria GE, Robb MA, Cheeseman JR, et al. Gaussian 09. Wallingford CT: Gaussian, Inc.; 2009.
[42] Van Speybroeck V, Van Neck D, Waroquier M, Wauters S, Saeys M, Marin GB. J Phys Chem A 2000;104:10939–50.
[43] (a) Gonzalez C, Schlegel HB. J Phys Chem 1990;94:5523–7;
(b) Gonzalez C, Schlegel HB. J Chem Phys 1989;90:2154–61.
[44] Theodorou DN, Suter UW. Macromolecules 1985;18:1467–78.
[45] Sun H. J Phys Chem B 1998;102:7338–64.
[46] Andersen HC. J Chem Phys 1980;72:2384–93.
[47] Atkins PW, De Paula J. Atkins' physical chemistry. New York: Oxford University Press; 2006.
[48] Liptak MD, Gross KC, Seybold PG, Feldgus S, Shields GC. J Am Chem Soc 2002;124:6421–7.